Stability and anomalous entropic elasticity of subisostatic random-bond networks

M. C. Wigbers,[1,*] F. C. MacKintosh,[1,†] and M. Dennison[1,2,‡]
[1]*Department of Physics and Astronomy, VU University, De Boelelaan 1081, 1081 HV Amsterdam, The Netherlands*
[2]*Department of Applied Physics and Institute for Complex Molecular Systems, Eindhoven University of Technology, P.O. Box 513, 5600 MB Eindhoven, The Netherlands*
(Received 30 October 2014; published 22 October 2015)

We study the elasticity of thermalized spring networks under an applied bulk strain. The networks considered are subisostatic random-bond networks that, in the athermal limit, are known to have vanishing bulk and linear shear moduli at zero bulk strain. Above a bulk strain threshold, however, these networks become rigid, although surprisingly the shear modulus remains zero until a second, higher, strain threshold. We find that thermal fluctuations stabilize all networks below the rigidity transition, resulting in systems with both finite bulk and shear moduli. Our results show a $T^{0.66}$ temperature dependence of the moduli in the region below the bulk strain threshold, resulting in networks with anomalously high rigidity as compared to ordinary entropic elasticity. Furthermore, we find a second regime of anomalous temperature scaling for the shear modulus at its zero-temperature rigidity point, where it scales as $T^{0.5}$, behavior that is absent for the bulk modulus since its athermal rigidity transition is discontinuous.

DOI: 10.1103/PhysRevE.92.042145 PACS number(s): 05.70.Jk, 62.20.de, 64.60.F−, 83.10.Tv

I. INTRODUCTION

Materials such as plastics and rubbers as well as tissues and living cells contain polymer networks, which, among other roles, provide structural support to these materials. Tissues and cellular networks are especially sensitive to external stresses [1–7] and a number of theoretical and simulation studies have attempted to gain an understanding of what controls the response of such systems to deformations [8,9]. Maxwell showed that there is a connectivity threshold z_c, determined by the average coordination number of the network nodes, at which athermal networks of springs become rigid [10]. This threshold, referred to as the isostatic point, occurs when the number of degrees of freedom of the network nodes is just balanced by the number of constraints arising from the springs. This purely mechanical argument has been used to describe the stability systems ranging from emulsions and jammed particle packings [11,12] to amorphous solids [13] and folded proteins [14]. Beyond this, theoretical work has shown that there are numerous ways of stabilizing a network, and therefore tuning its rigidity, below the isostatic point [15]. Examples include the addition of a bending stiffness to the model filaments [16–18] by applying stress [19] either internally via molecular motors [20,21] or externally by placing the network under tension by applying a bulk strain to the system [22–24]. It has been shown that a network's rigidity point can be shifted from the Maxwell point by adding these interactions and forces to the system. In the case of applying a bulk strain [22–24] the system can be stabilized by stretching the network until all the floppy modes have been pulled out, resulting in a critical strain at which the network is just rigid. Here the network will only become mechanically floppy at the percolation point, where there is no longer a connected path through the system [23].

In addition to these athermal models, recent work has shown how temperature can stabilize a mechanically floppy network [25–30]. In Ref. [29] it was found that at and below the isostatic point the network response to deformation, defined by the shear modulus, not only becomes finite when thermal fluctuations are present, but also shows an anomalous temperature scaling of T^{α}, where $\alpha < 1$. This sublinear temperature dependence indicates that a network would exhibit a *larger* resistance to deformation than would be expected from entropic elasticity, where one would expect a linear temperature dependence [31]. The origin of this anomalous temperature dependence remains unclear and in addition there have been few studies into the effects of thermal fluctuations on subisostatic networks [25,32–34]. Furthermore, in Ref. [29] a triangular-lattice-based network was used and an open question is how general the anomalous regimes found are, since network architecture can have vast effects on a system's response to deformation [35,36]. Indeed, in Ref. [30] a square lattice (which is at the isostatic point) with next-nearest-neighbor interactions was found to stiffen with a different critical exponent than a randomly diluted triangular lattice also at the isostatic point [29].

In this paper we study the effects of thermal fluctuations on an underconstrained and mechanically floppy random-bond network. The architecture of a random-bond network is as different as possible from a triangular-lattice network, as the nodes are arranged isotropically and there is a distribution of filament lengths. The random-bond model proposed by Jacobs and Thorpe [37] has been used previously to study the effects of applying a bulk strain on the rigidity of athermal networks [24]. The connectivity threshold for rigidity percolation of this model will be somewhat lower than that of a lattice network [38,39].

In addition, we study the dependence of the internal pressure, bulk modulus, and shear modulus of a random-bond network with average coordination number $z = 3$ on the bulk strain and temperature. This coordination number lies between the connectivity percolation threshold (below

*Present address: Department of Physics, Ludwig-Maximilians-Universität München, Theresienstrasse 37, D-80333 München, Germany; Theory of Complex Biosystems, Physik-Department, Technische Universität München, James-Franck-Strasse 1, 85748 Garching, Germany; m.wigbers@campus.lmu.de
†fcmack@gmail.com
‡Present address: Institut für Theoretische Physik, Technische Universität Berlin, Hardenbergstraße 36, 10623 Berlin, Germany; matthew.dennison@yahoo.co.uk

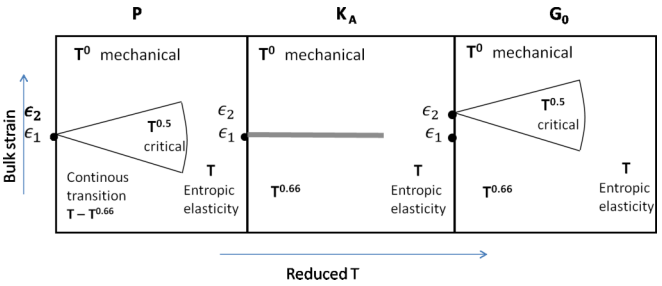

FIG. 1. (Color online) Schematic phase diagram showing behavior of the internal pressure P, bulk modulus K_A, and shear modulus G with bulk strain ϵ and temperature T for subisostatic random-bond networks with connectivity $z = 3$.

which the networks would be floppy regardless of strain or thermal fluctuations [19,24]) and the isostatic threshold for central-force interactions (above which athermal spring networks become rigid [10]).

We show that, as reported previously in Ref. [24], there exists a bulk strain threshold at which the system will begin to resist bulk deformations at zero temperature. However, the network does not begin to resist shear deformation until a second, higher, strain threshold is reached and it is these two thresholds that control the network response to the applied deformations. We find anomalous scaling regimes for the shear modulus at and below its threshold, similar to the results of Ref. [29], where the bulk strain applied to the networks in this study takes on a similar role to the connectivity in Ref. [29]. Interestingly, we find that, while the bulk modulus exhibits a similar anomalous scaling regime below its threshold, we find no temperature dependence at its strain threshold, at which there is a first-order zero-temperature rigidity transition. The network behavior is summarized in the phase diagrams shown in Fig. 1.

II. PHYSICAL PICTURE

Since Maxwell [10] it has been known that an athermal network of central-force springs will be floppy below a critical, isostatic connectivity threshold. This means that there is no energy cost for small bulk or shear deformations. When applying an increasingly large uniform bulk strain, such networks will begin to resist additional bulk deformations at a strain threshold corresponding to a rigidity transition [24], at which the network will be just rigid. Applying small deformations on a rigid network will cost energy, since the springs will be stretched, which results in a stable network exhibiting a nonzero bulk modulus at zero temperature.

A mechanically floppy network will also be stabilized by thermal fluctuations [25,29]. The resulting network is rigid both above *and* below the rigidity point. A deformation of a mechanically floppy network results in a reduction of the number of microstates that the system can assume, even though the system energy remains unchanged. This results in a change in entropy as the system is deformed, which gives rise to a change in the free energy, resulting in nonzero elastic moduli at finite temperatures. Thus, below the rigidity point the network is stabilized by thermal fluctuations, as the entropic contribution to the moduli dominates the mechanical contribution. When the network is sufficiently stretched, i.e., above the bulk strain rigidity threshold, all springs are under tension that causes the mechanical stretching energy (controlled by the spring constant) to dominate the thermal fluctuations in stabilizing the network and the network rigidity then becomes independent of temperature. As thermal networks are always rigid, there is no bulk strain threshold at which the network becomes stable. However, if a network is taken to the rigidity point, we find that there can be an anomalous intermediate regime in which the network is stabilized by both temperature and the spring constant.

These three different regimes of network stability are defined by the bulk strain at the zero-temperature rigidity transition. This strain depends on how constrained the system is, controlled, for example, by varying the connectivity of the network by changing the number of springs. Lowering the connectivity will lower the number of constraints in the network and it has been shown that subisostatic networks with increasingly lower connectivities need to be increasingly stretched to become rigid [24].

III. MODEL

In this paper we study the effects of thermal fluctuations and bulk strain on the stability of subisostatic random-bond networks. The random-bond network is constructed by placing N nodes randomly in a two-dimensional box of area A, which are then connected by $N_{\rm sp}$ springs until the network reaches an average connectivity $z = 2N_{\rm sp}/N$ [24,37]. Since unconnected nodes will not contribute to the networks response, each node is first connected to at least one randomly chosen other node. Thus, our networks are random, in that both the positions of the nodes and the length of the connecting springs are random. Periodic boundary conditions are used throughout and the springs may cross the system boundaries. Furthermore, we do not allow two nodes to be connected by more than one spring or both ends of the spring to connect to the same node. This method would still allow for disconnected clusters to form. While this method does not generate a truly random network, we find that in practice this does not effect the results we present in this paper, as will be shown. A schematic of a random-bond network is shown in Fig. 2. The springs have a rest length l_0, which will vary for each spring and, by construction, the average rest length will be half the system size. We use the average spring length $\langle l_0 \rangle$ as the unit of length and we note that for systems with the same density

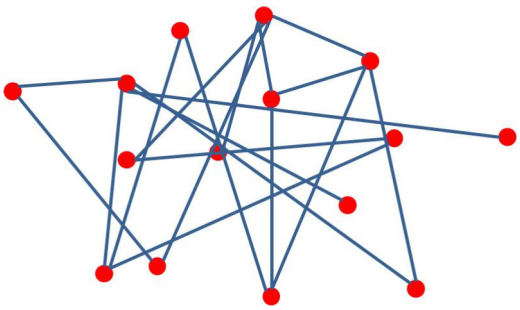

FIG. 2. (Color online) Schematic representation of a random-bond network. The network is constructed by placing N nodes randomly in a box. The nodes are randomly connected by $zN/2$ springs to reach an average connectivity z.

of nodes $\langle l_0 \rangle$ grows as $\sqrt{N}$ and as such there is no well defined thermodynamic limit. In this simple model the only two energy scales are the stretching energy and the thermal energy. The total energy of the network is given by the sum of the energy of all $N_{\rm sp}$ springs

$$U = \frac{k_{\rm sp}}{2} \sum_{i}^{N_{\rm sp}} \langle l_i - l_{0,i} \rangle^2, \tag{1}$$

where $k_{\rm sp}$ is the spring constant and $l_{0,i}$ the rest length of spring i, which has length

$$l_i = \sqrt{(x_2 - x_1)^2 + (y_2 - y_1)^2}, \tag{2}$$

where x_j and y_j are the coordinates of nodes $j = 1,2$ that are connected by spring i. To study fiber networks, it is common to set the spring constant to $k_{{\rm sp},i} = \mu / l_{0,i}$ [16–18,35,36,40,41], where μ is the one-dimensional Young (stretch) modulus. This means that long springs will become progressively weaker and contribute less to the network response. For polymers, flexible or semiflexible, yet a different length dependence is possible [2,42–44]. We choose to keep the spring constant identical for each spring, as we find that this has no qualitative effect on our results (see Fig. 3) and speeds up our computer simulations.

This network architecture is isotropic and differs qualitatively from a lattice-based network, for which the springs have either the same length or a narrow discontinuous distribution of lengths. In the random-bond network, there are springs with lengths of the order of the system size, which would prevent network collapse at finite temperature due to entropic forces [29,45]. Thus, the random-bond model is stable to thermal fluctuations without an imposed tension at the boundaries. We have chosen this minimalist off-lattice network in order to study the anomalous low-temperature behavior found in lattice networks [29]. However, whereas this network is most different from a lattice network, it shows some similar behavior to temperature. It is deliberately highly theoretical and does not represent a real system, but does let us examine the anomalous temperature dependence in detail.

In order to study the entropic stabilization, we apply varying bulk strains to the system by uniformly scaling the system area such that

$$A = A_0(1 + \epsilon)^2, \tag{3}$$

where A_0 is the rest area of a fully relaxed network at temperature $T = 0$ and ϵ is the applied strain. The x and y coordinate of each node are also scaled, defining new coordinates x' and y' for node j as

$$x'_j = x_j(1 + \epsilon). \tag{4}$$

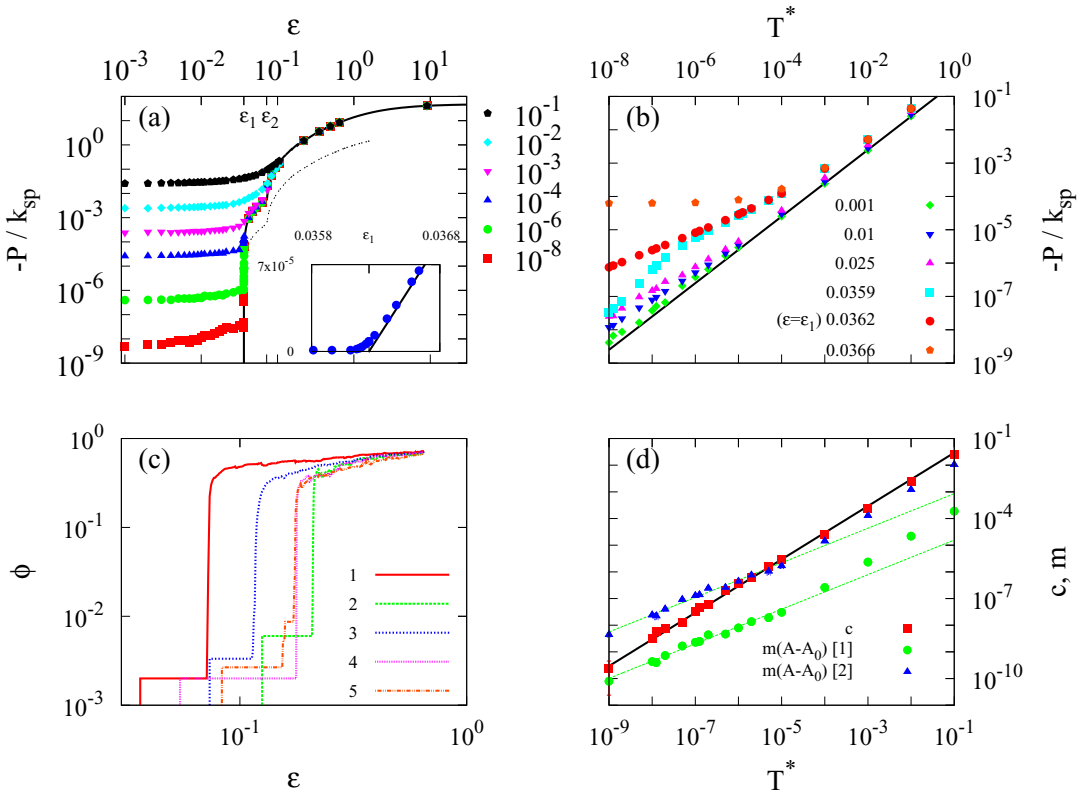

FIG. 3. (Color online) Pressure P of the random-bond spring network with $N = 1000$ nodes against (a) bulk strain ϵ and (b) reduced temperature $T^* = k_B T / k_{\rm sp} \langle l_0 \rangle^2$. (a) The solid line shows the zero-temperature behavior, points are for thermal systems, and the dashed line shows results for the same system but with the spring constant of individual springs given by $k_{{\rm sp},i} = \mu / l_{0,i}$, where μ is a stretch modulus. (b) The solid line shows linear T dependence. (c) Fraction of stretched springs ϕ in the network as a function of ϵ for five different network configurations. (d) Behavior of m and c for the function $-P = m(A - A_0) + c$ with reduced temperature T^*, where A is the area and A_0 is the rest area at $\epsilon = 0$. The solid black line shows the linear T dependence, dashed green lines show $T^{0.66}$ dependence. [1] indicates $\epsilon = 0.03$ and [2] indicates $\epsilon = 0.001$.

That is, the network is stretched uniformly and after this affine deformation the system is allowed to relax nonaffinely. We introduce the temperature T using Monte Carlo simulations to study the equilibrium behavior of thermal systems.

Elastic moduli and internal pressure

We determine the internal pressure and bulk modulus of the system under bulk strain. The internal pressure is defined as

$$P = -\frac{\partial F}{\partial A}, \tag{5}$$

where F is the Helmholtz free energy, and can be calculated in our simulations as [46]

$$P = \frac{N}{A}k_B T + \frac{1}{2A}\sum_{i}^{N}\sum_{j}^{N}\langle f_{i,j} l_{i,j}\rangle$$

$$= \frac{N}{A}k_B T - \frac{1}{2A}\sum_{k}^{N_{\rm sp}}\langle k_{\rm sp} l_k (l_k - l_0)\rangle, \tag{6}$$

where the first line contains a sum over all pairs of nodes and the second line contains a sum over all springs, since the force $f_{i,j}$ between node i and node j is only nonzero if there is a spring connecting i and j. The first term represents the ideal gas behavior and the second term corrects for spring interactions. By calculating the internal pressure at various areas we can then calculate the bulk modulus, which is defined by

$$K_A = -A\frac{\partial P}{\partial A}. \tag{7}$$

In addition, we calculate the shear modulus G of the networks at each bulk strain; G is defined by

$$G = \frac{1}{A}\frac{\partial^2 F}{\partial \gamma^2}, \tag{8}$$

where γ is the shear strain. In order to shear the network we use Lees-Edwards boundary conditions [47], where the energy of the springs crossing the top boundary of the simulation box is modified to become

$$E_{\rm sp}(l) = \frac{k_{\rm sp}}{2}[\sqrt{(x_{ij} + \gamma L_y)^2 + (y_{ij})^2} - l_0]^2, \tag{9}$$

where L_y is the height of the simulation box. As for the bulk strain, we first affinely deform the network and let the system relax, allowing nonaffine deformations. We initially shear the networks at zero temperature, obtaining a configuration under shear, and then increase the temperature from zero. For these thermal systems, we calculate the shear stress σ as in Refs. [29,48]. The shear modulus can then be calculated by taking the derivative of the stress on the network with respect to γ at $\gamma = 0$.

IV. RESULTS

We calculate the pressure, bulk modulus, and shear modulus for two-dimensional random-bond networks with a connectivity of $z = 3$ over a range of reduced temperatures $T^* = k_B T/k_{\rm sp}\langle l_0\rangle^2$ and bulk strains ϵ. For these systems, the critical connectivity is $z_c \sim 4$. Thus, our networks are subisostatic and will be floppy at $T = 0$ and $\epsilon = 0$. Results for the pressure are presented in Fig. 3, for the bulk modulus in Fig. 4, and for the shear modulus in Fig. 5. We first examine in detail the behavior of the properties related to bulk deformation, i.e., the pressure and bulk modulus, before examining the behavior of the shear modulus.

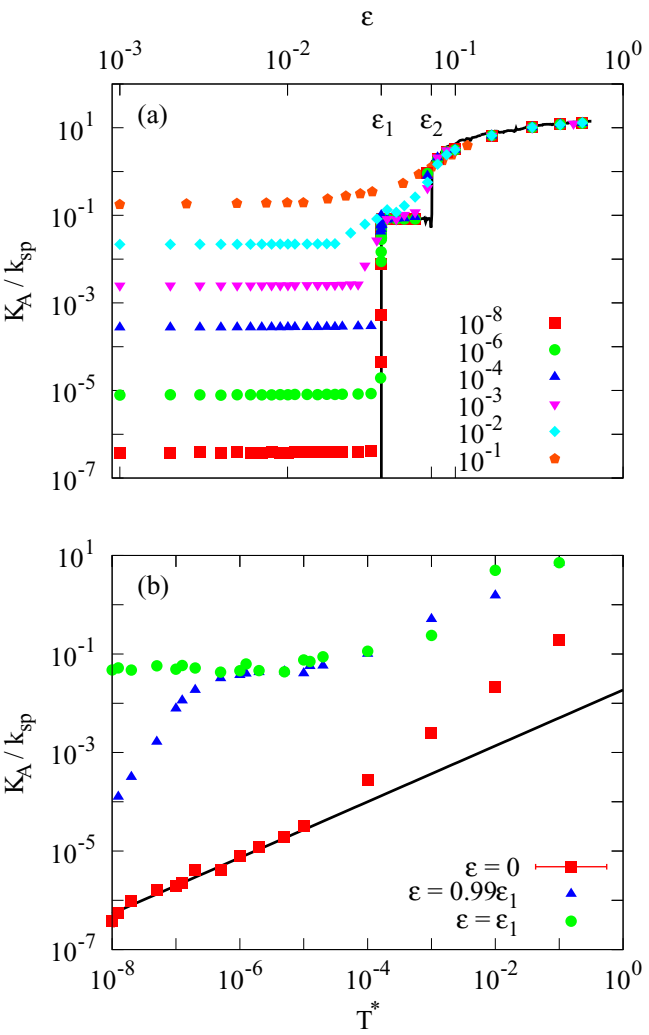

FIG. 4. (Color online) Bulk modulus K_A of the random-bond spring network with $N = 1000$ nodes against (a) bulk strain ϵ and (b) reduced temperature $T^* = k_B T/k_{\rm sp}\langle l_0\rangle^2$. (a) The solid line shows the zero-temperature behavior and points are for thermal systems. (b) The solid line shows the $T^{0.66}$ dependence.

At zero temperature we find a strain ϵ_1 (with corresponding area A_1) at which the network just becomes rigid, indicated by the solid black line in Figs. 3(a) and 4(a). Here the network exhibits a finite pressure and bulk modulus above ϵ_1, and zero pressure and bulk modulus below, and we hence define this strain threshold as the rigidity point. The pressure shows a linear dependence on area, increasing continuously as $-P = c_1(A - A_1)$ for $A \geqslant A_1$, where c_1 is a constant. Based on the definition of the bulk modulus given in Eq. (7) this means that $K_A = c_1 A$ for $A \geqslant A_1$ and $K_A = 0$ for $A < A_1$, i.e., a discontinuous increase in K_A, corresponding to a first-order transition from a floppy to a rigid network at ϵ_1. We note that the value of ϵ_1 will differ for different network configurations, as there is no well defined thermodynamic limit for random-bond networks due to the average spring length

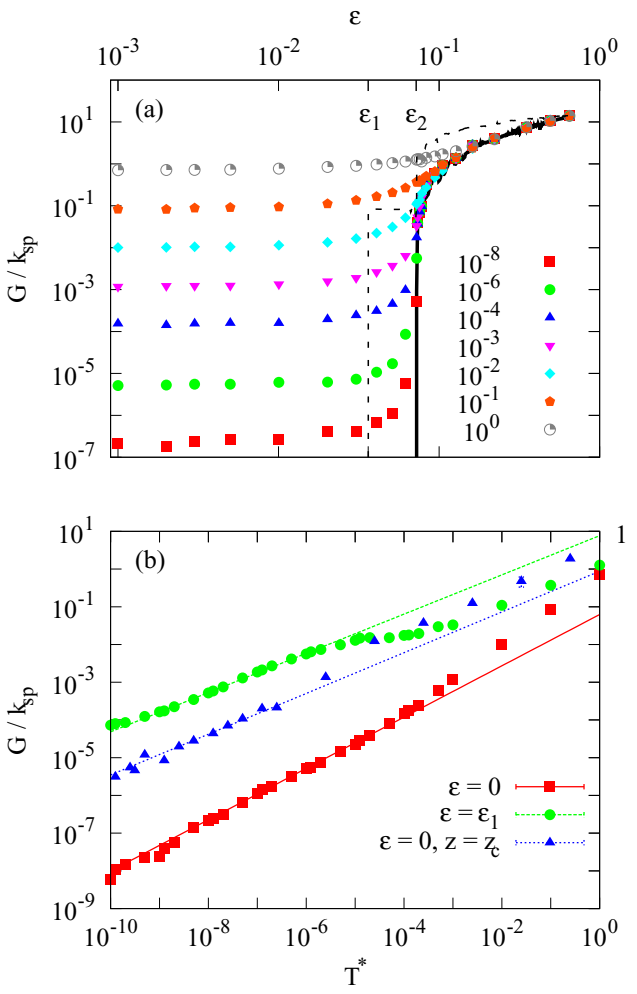

FIG. 5. (Color online) Shear modulus G of the random-bond spring network with $N = 1000$ nodes against (a) bulk strain ϵ and (b) reduced temperature $T^* = k_B T / k_{sp} \langle l_0 \rangle^2$. (a) The solid line shows the zero-temperature behavior, while points are for thermal systems. The dashed line shows the bulk modulus K_A for the same system at zero temperature. (b) The solid red line shows the $T^{0.66}$ dependence while dotted blue and green lines show the $T^{0.5}$ dependence. Red squares and green circles show data for a network with $z = 3$ at a bulk strain ϵ indicated in the legend, while blue triangles show data for a network at $z = z_c$ and $\epsilon = 0$.

growing with the system size. The response of the networks to bulk strain or thermal fluctuation does not differ between different configurations with the same average conductivity. For the results presented in Figs. 3(a) and 4(a) a network with $\epsilon_1 = 0.0356$ was used. The first-order nature of the transition was present in all configurations studied.

When thermal fluctuations are present the network is rigid for all bulk strains, as can be seen in Figs. 3(a) and 4(a) where different temperatures are represented by the colored points. For small bulk strains ($\epsilon < \epsilon_1$) the network is stabilized by the thermal fluctuations and exhibits an increasingly large pressure and bulk modulus as the temperature is increased. As ϵ_1 is approached we observe a regime where the pressure and bulk modulus for all temperatures start to join the zero-temperature line, with the low-temperature results starting to join the zero-temperature result sooner than the results for higher temperatures. For bulk strains greater than ϵ_1 there is a mechanical regime, where tension is dominant over thermal fluctuations and the resistance to deformation depends only on the spring constant. However, we find that the pressure no longer increases linearly with area as ϵ_1 is approached, even at low temperatures [see the inset of Fig. 3(a)], resulting in a continuous transition between the thermal-dominated regime and the mechanical regime.

In Figs. 3(b) and 4(b) we show the temperature dependence of the internal pressure and bulk modulus in the thermal, intermediate, and mechanical regimes. Above ϵ_1 we find that they are both independent of temperature; in this mechanical regime the network is completely stabilized by the spring constant and its response to deformation is invariant to temperature. At and below the rigidity point the temperature dependence becomes more complex. Below ϵ_1 the pressure in the network scales as $P \propto T^\alpha$. When the network is at zero strain $\epsilon = 0$ we find that $\alpha = 1$, as expected in analogy to entropic elasticity [31]. However, as the strain is increased we find $\alpha \lesssim 1$, with an exponent that decreases as the strain is increased, reaching $\alpha \sim 0.66$ as the critical strain is approached. We observe this dependence only at low temperatures $T^* < 10^{-5}$, with the pressure scaling linearly at higher temperatures. This varying temperature dependence of the pressure can be understood when we consider the behavior of pressure in the initial linear response regime. That is, at low bulk strains we find that the pressure scales linearly with area and at low temperatures can be expressed as $-P = m(T)(A - A_0) + c(T)$, where $m(T)$ and $c(T)$ are constants for a given temperature T. It then follows that the bulk modulus will scale as $K_A = m(T)A$. By fitting this expression for the pressure to our simulation data we find that $m(T) \propto T^{0.66}$ (for $T^* < 10^{-5}$) and $c(T) \propto T$, as shown in Fig. 3(d). Hence, at low bulk strains ($A \sim A_0$) $c(T)$ dominates and we find a linear temperature dependence, while at higher bulk strains the system approaches a regime where $m(T)(A - A_0)$ dominates $c(T)$ and we hence observe a $T^{0.66}$ dependence, with a mixed regime between the two. The bulk modulus then scales with $T^{0.66}$ for all $\epsilon < \epsilon_1$ at low T^* and linearly at higher temperatures. On dimensional grounds it follows that the pressure and bulk modulus must also have a dependence on the spring constant and scale as $P, K_A \propto T^\alpha k_{sp}^{1-\alpha}$.

For bulk strains close to ϵ_1, we find that P scales with the square root of temperature $P \propto T^{0.5}$ for $T^* < 10^{-5}$ and linearly with temperature for $T^* > 10^{-5}$, as shown in Fig. 3(b). In the $T^{0.5}$ regime the network is again stabilized by both temperature and the spring constant and we find that P scales as $T^{0.5} k_{sp}^{0.5}$. We also observe that networks below the rigidity point can enter this regime as the temperature is increased. For these systems the pressure initially shows a $T^{0.66}$ dependence before they then show a $T^{0.5}$ dependence, indicating a regime that fans out from the zero-temperature rigidity point. The bulk modulus, however, exhibits a different behavior in this region, as for networks at ϵ_1 we find that K_A is independent of temperature. For networks just below this point we observe a rapid increase in the modulus with T, before K_A reaches the zero-temperature value.

As the area is increased for $\epsilon > \epsilon_1$, there is a clear inflection point in the zero-temperature (and low-temperature) pressure,

as can be seen in Fig. 3(a). At this point the pressure again increases linearly with area as $-P = c_2(A - A_2)$, where c_2 and A_2 are larger than c_1 and A_1, respectively. This corresponds to a reorganization of the network, as the nodes change positions to minimize the system energy. This is illustrated in Fig. 3(c), where we plot the fraction of springs in the network that are *activated* (i.e., stretched or compressed such that $l \neq l_0$). At ϵ_1 we see the first springs become activated, followed by a significant jump at a higher value of ϵ. Furthermore, as the area is increased beyond this point, we find several more reorganizations, as can be seen by the kinks in Fig. 3(c) [there are also further kinks in the pressure in Fig. 3(a), although these are not visible on the logarithmic scale used]. This is present for all configurations and system sizes studied and in Fig. 3(c) we present data from additional configurations to illustrate this. This effect is also present when we take the spring constant of individual springs to be given by $k_{\mathrm{sp},i} = \mu / l_{0,i}$, where μ is a stretch modulus [see Fig. 3(a)], such that very long springs will become progressively weaker and contribute less to the network response. This is likely due to the fact that it is neither the very long nor very short springs that dominate the system's response as the network is stretched beyond its rigidity point, which we confirm by examining the rest lengths of the activated springs in Fig. 3(c). The effect that the reorganization of the network has on the bulk modulus can be seen in Fig. 4(a), where we see that there is a second distinct jump in K_A, corresponding to a first-order transition as the system rearranges, with further jumps present at higher areas, although again these are not visible on the logarithmic scale used.

We now examine the behavior of the linear shear modulus G, which we obtained by shearing the networks at each bulk strain. For athermal networks G is zero at low bulk strains, as one would expect for a floppy network before any of the springs become stretched. However, the shear modulus remains zero beyond ϵ_1, with the network not resisting shear deformation until it reaches a bulk strain $\epsilon = \epsilon_2$ [see Fig. 5(a)]. This strain corresponds to that at which we observed the second jump in the bulk modulus as shown in Fig. 5(a). Beyond this point the shear modulus increases linearly with the area and the network becomes rigid to shear deformation, indicating a continuous transition in G. As for the pressure and bulk modulus, when thermal fluctuations are present we find a nonzero shear modulus throughout, with thermal, intermediate, and mechanical regimes present, although here the intermediate regime is found at ϵ_2. The different regimes can be seen in Fig. 5, where we see G remaining constant with temperature above ϵ_2 and G scaling with T^α at and below ϵ_2, with $\alpha \sim 0.66$ below and $\alpha \sim 0.5$ in the intermediate regime.

The temperature dependence of the different regimes of behavior for the pressure and shear modulus can be captured by a crossover scaling technique similar to that used for the conductivity of a random resistor network [49]. This technique has been used previously to describe the shear modulus for both athermal [15,18] and thermal systems [29]. The scaling forms are given by

$$G = |\epsilon - \epsilon_2|^a \mathcal{G}(T|\epsilon - \epsilon_2|^{-b}) \tag{10}$$

and

$$P = |\epsilon - \epsilon_1|^k \mathcal{P}(T|\epsilon - \epsilon_1|^{-l}), \tag{11}$$

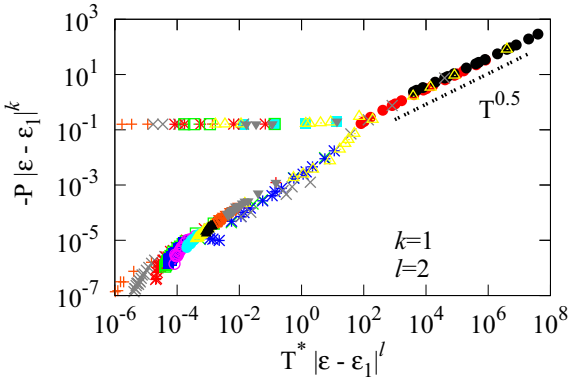

FIG. 6. (Color online) Scaling of the pressure P using the form $P = |\epsilon - \epsilon_1|^k \mathcal{P}(T|\epsilon - \epsilon_1|^{-l})$, where $k = 1$ and $l = 2$ are constants that give the best collapse of data. The two branches on the left-hand side correspond to $\epsilon > \epsilon_1$ (upper branch) and $\epsilon < \epsilon_1$ (lower branch).

where a/b and k/l are the exponents in the intermediate regime for, respectively, the shear modulus and pressure. The best collapses of the data are shown in Figs. 6 and 7, where we use the critical exponents $a,k = 1$ and $b,l = 2$. The two collapses summarize the three regimes of network stability. The upper left branches show the mechanical regimes, the lower left branch shows the temperature dominated regime, where we find a $T^{0.66}$ dependence for the shear modulus and the varying T dependences for the pressure, and the right branch shows the intermediate regime, where we find a temperature dependence of $T^{0.5}$ for both G and P.

V. DISCUSSION AND IMPLICATION

The behavior of the subisostatic random-bond networks considered in this paper is similar to the behavior found in Ref. [29] for lattice-based networks. The observed sublinear scaling of the shear modulus $G \propto T^\alpha$ for networks below the critical bulk strain was also found for lattice-based networks, albeit with different exponents, with $\alpha \sim 0.66$ for the random-bond networks studied here and $\alpha \sim 0.8$ for the triangular-lattice networks studied in Ref. [29]. This indicates that, while sublinear scaling is not confined to lattice models, the exponent

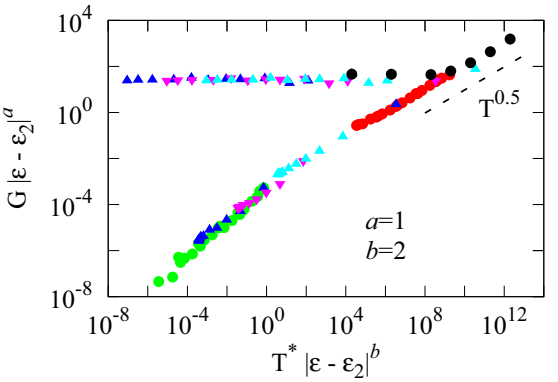

FIG. 7. (Color online) Scaling of the shear modulus G using the form $G = |\epsilon - \epsilon_2|^a \mathcal{G}(T|\epsilon - \epsilon_2|^{-b})$, where $a = 1$ and $b = 2$ are constants that give the best collapse of data. The two branches on the left-hand side correspond to $\epsilon > \epsilon_2$ (upper branch) and $\epsilon < \epsilon_2$ (lower branch).

does depend on the topology of the network. Indeed, in a recent paper [30] it was found that a square-lattice network with next-nearest-neighbor interactions, which is at the isostatic point when the next-nearest-neighbor interactions are zero, showed a critical regime where $G \propto T^{\alpha}$ with $\alpha \sim 0.66$, different from the $\alpha \sim 0.5$ observed both in Ref. [29] for a diluted-triangular-lattice network at the isostatic point and in the random-bond networks presented here (see Fig. 5). We do, however, find the same temperature dependence of a random-bond network at the isostatic point as the diluted-triangular-lattice network, with $\alpha \sim 0.5$ at $z = z_c$.

In Ref. [29] it was proposed that the scaling may be due to the internal pressure P, which at $\epsilon = 0$ scales linearly with temperature, leading to $G \propto k_{\mathrm{sp}}^{0.2} P^{0.8}$. This was in analogy to a study on athermal networks with an internal stress σ_m induced by molecular motors, where $G \sim k_{\mathrm{sp}}^{0.2} \sigma_m^{0.8}$ below the isostatic point [21]. However, as we find that the pressure begins to scale sublinearly with temperature as the bulk strain is increased from $\epsilon = 0$ while the $G \propto T^{\alpha}$ scaling remains, this proposed scaling would not be valid as one moves away from the rest area of the network at $\epsilon \neq 0$. Indeed, the shear modulus shows the same temperature dependence as the bulk modulus, which scales as $K_A = m(T)A$, where $m(T) \sim T^{0.66}$ was obtained from the relation for the pressure $-P = m(T)(A - A_0) + c(T)$.

In addition to the similarities between the behavior found here for subisostatic, subcritical random-bond networks and subisostatic lattice-based networks, we also note the similarities between the behavior of networks at the bulk strain threshold corresponding to the rigidity point and networks at the critical connectivity z_c. In Ref. [29] it was found that the shear modulus behaved as $G \propto T^{0.5}$ at z_c (at the critical connectivity the critical strain is zero $\epsilon_c = 0$ [24]), indicating that the stabilization of the network at the critical strain is similar to that at z_c. We note that this is only true of the shear modulus, as we find a constant bulk modulus for low temperatures at ϵ_1. A possible reason for the differences in the observed temperature dependence between the two moduli would be the nature of the zero-temperature transition from zero to finite modulus, as the bulk modulus exhibits a first-order transition at ϵ_1 while the shear modulus exhibits a continuous transition at ϵ_2. We also note that the exponents found for the crossover scaling ansatz in Eq. (10), $a = 1$ and $b = 2$, are more mean-field-like than those found for the critical connectivity case [18,29].

Finally, the zero-temperature behavior of the random-bond networks considered here differs greatly from that of lattice-based networks, exhibiting a noncontinuous transition from a floppy to a rigid network as the bulk strain is increased [24] and exhibiting a regime where the system has a finite bulk strain but zero shear modulus. However, despite these differences in the athermal behavior, as previously mentioned the temperature dependence of the thermal stiffening of the network does not change qualitatively [29].

VI. CONCLUSION

In this paper we have studied the effects of thermal fluctuations on the elastic response of random-bond networks at various bulk strains. Our results show that, in agreement with previous studies, there is a bulk strain threshold at zero temperature for which the bulk modulus and pressure of a floppy network will become finite. We find that the transition for the pressure is continuous while it is discontinuous for the bulk modulus, jumping to a finite value at the rigidity point. We have also found that random-bond networks can exhibit further discontinuous transitions, as the networks rearrange to minimize their energy. Unusually, the random-bond networks studied here exhibit a regime where there is a finite bulk modulus but zero shear modulus at zero temperature. In these systems, the bulk strain threshold for a nonzero shear modulus is larger than that for a nonzero bulk modulus and the shear modulus transitions continuously at its rigidity point.

When thermal fluctuations are present the network becomes stable for all strains and the pressure and bulk modulus transition continuously between a thermally dominated regime and a mechanical regime at the zero-temperature rigidity, while the shear modulus transitions continuously at its own bulk strain threshold. In between these two regimes, there exists a third, intermediate, regime where the pressure and shear modulus depend on the square root of temperature (at their respective strain thresholds) while the bulk modulus remains constant, as the intermediate scaling occurs only at a continuous rigidity transition. Perhaps most interestingly, we find that the shear and bulk moduli exhibit an anomalous temperature scaling of T^{α} with $\alpha \sim 0.66$ below the critical strain, where we would expect to find normal entropic elasticity (linear temperature scaling $\approx T$). This behavior is similar to that reported in Ref. [29], where the shear modulus was found to scale as $T^{0.8}$, indicating that floppy networks of various topologies can exhibit anomalous temperature scaling.

ACKNOWLEDGMENTS

This work was supported in part by the Foundation for Fundamental Research on Matter (FOM), which is part of the Netherlands Organization for Scientific Research (NWO). We thank A. Licup, A. Sharma, M. Sheinman, and C. Storm for many discussions.

[1] Y. C. B. Fung, Am. J. Physiol. **213**, 1532 (1967).
[2] M. L. Gardel, J. H. Shin, F. C. MacKintosh, L. Mahadevan, P. Matsudaira, and D. A. Weitz, Science **304**, 1301 (2004).
[3] C. Storm, J. J. Pastore, F. C. MacKintosh, T. C. Lubensky, and P. A. Janmey, Nature (London) **435**, 191 (2005).
[4] M. Gardel, F. Nakamura, J. Hartwig, J. Crocker, T. Stossel, and D. Weitz, Proc. Natl. Acad. Sci. USA **103**, 1762 (2006).
[5] C. P. Broedersz, C. Storm, and F. C. MacKintosh, Phys. Rev. Lett. **101**, 118103 (2008).
[6] K. E. Kasza, G. H. Koenderink, Y. C. Lin, C. P. Broedersz, W. Messner, F. Nakamura, T. P. Stossel, F. C. MacKintosh, and D. A. Weitz, Phys. Rev. E **79**, 041928 (2009).
[7] Y.-C. Lin, N. Y. Yao, C. P. Broedersz, H. Herrmann, F. C. MacKintosh, and D. A. Weitz, Phys. Rev. Lett. **104**, 058101 (2010).

[8] A. R. Bausch and K. Kroy, Nat. Phys. **2**, 231 (2006).
[9] C. P. Broedersz and F. C. MacKintosh, Rev. Mod. Phys. **86**, 995 (2014).
[10] J. C. Maxwell, Philos. Mag. **27**, 294 (1864).
[11] M. van Hecke, J. Phys.: Condens. Matter **22**, 033101 (2010).
[12] A. J. Liu and S. R. Nagel, Annu. Rev. Condens. Matter Phys. **1**, 347 (2010).
[13] L. Golubović and T. C. Lubensky, Phys. Rev. Lett. **63**, 1082 (1989).
[14] A. J. Rader, B. M. Hespenheide, A. L. Kuhn, and M. F. Thorpe, Proc. Natl. Acad. Sci. USA **99**, 3540 (2002).
[15] M. Wyart, H. Liang, A. Kabla, and L. Mahadevan, Phys. Rev. Lett. **101**, 215501 (2008).
[16] D. A. Head, A. J. Levine, and F. C. MacKintosh, Phys. Rev. Lett. **91**, 108102 (2003).
[17] J. Wilhelm and E. Frey, Phys. Rev. Lett. **91**, 108103 (2003).
[18] C. P. Broedersz, T. C. Lubensky, X. Mao, and F. C. MacKintosh, Nat. Phys. **7**, 983 (2011).
[19] S. Alexander, Phys. Rep. **296**, 65 (1998).
[20] C. P. Broedersz and F. C. MacKintosh, Soft Matter **7**, 3186 (2011).
[21] M. Sheinman, C. P. Broedersz, and F. C. MacKintosh, Phys. Rev. Lett. **109**, 238101 (2012).
[22] W. Tang and M. F. Thorpe, Phys. Rev. B **36**, 3798 (1987).
[23] W. Tang and M. F. Thorpe, Phys. Rev. B **37**, 5539 (1988).
[24] M. Sheinman, C. P. Broedersz, and F. C. MacKintosh, Phys. Rev. E **85**, 021801 (2012).
[25] M. Plischke and B. Joós, Phys. Rev. Lett. **80**, 4907 (1998).
[26] O. Farago and Y. Kantor, Europhys. Lett. **52**, 413 (2000).
[27] O. Farago and Y. Kantor, Phys. Rev. Lett. **85**, 2533 (2000).
[28] O. Farago and Y. Kantor, Europhys. Lett. **57**, 458 (2002).
[29] M. Dennison, M. Sheinman, C. Storm, and F. C. MacKintosh, Phys. Rev. Lett. **111**, 095503 (2013).
[30] X. Mao, A. Souslov, C. I. Mendoza, and T. C. Lubensky, Nat. Commun. **6**, 5968 (2015).
[31] P.-G. de Gennes, *Scaling Concepts in Polymer Physics* (Cornell University Press, Ithaca, 1979).
[32] M. Rubinstein, L. Leibler, and J. Bastide, Phys. Rev. Lett. **68**, 405 (1992).
[33] B. Barrière, J. Phys. (France) I **5**, 389 (1995).
[34] F. Tessier, D. H. Boal, and D. E. Discher, Phys. Rev. E **67**, 011903 (2003).
[35] C. Heussinger and E. Frey, Phys. Rev. Lett. **96**, 017802 (2006).
[36] C. Heussinger and E. Frey, Phys. Rev. E **75**, 011917 (2007).
[37] D. J. Jacobs and M. F. Thorpe, Phys. Rev. Lett. **80**, 5451 (1998).
[38] O. Rivoire and J. Barré, Phys. Rev. Lett. **97**, 148701 (2006).
[39] S. P. Kasiviswanathan, C. Moore, and L. Theran, *Proceedings of the 22nd Annual ACM-SIAM symposium on Discrete Algorithms* (SIAM, Philadelphia, 2011), pp. 1237–1252.
[40] C. P. Broedersz, M. Sheinman, and F. C. MacKintosh, Phys. Rev. Lett. **108**, 078102 (2012).
[41] E. Conti and F. C. MacKintosh, Phys. Rev. Lett. **102**, 088102 (2009).
[42] F. C. MacKintosh, J. Kas, and P. A. Janmey, Phys. Rev. Lett. **75**, 4425 (1995).
[43] E. M. Huisman, C. Storm, and G. T. Barkema, Phys. Rev. E **78**, 051801 (2008).
[44] E. M. Huisman and T. C. Lubensky, Phys. Rev. Lett. **106**, 088301 (2011).
[45] D. H. Boal, U. Seifert, and J. C. Shillcock, Phys. Rev. E **48**, 4274 (1993).
[46] G. Jackson and E. de Miguel, J. Chem. Phys. **125**, 164109 (2006).
[47] A. W. Lees and S. F. Edwards, J. Phys. C **5**, 1921 (1972).
[48] D. R. Squire, A. C. Holt, and W. G. Hoover, Physica **42**, 388 (1969).
[49] J. Straley, J. Phys. C **9**, 783 (1976).